Rotavirus infection induces both interferon (IFN) and inflammatory resistance by re-programming intestinal IFN receptor signaling

Adrish Sen[1,2], Nima D. Namsa[1, 2, 3], Ningguo Feng[1,2], Harry B. Greenberg[1,2]

The Department of Microbiology and Immunology, Stanford University School of Medicine, Stanford, California, USA[1]; VA Palo Alto Health Care System, Palo Alto, California, USA[2], Department of Molecular Biology and Biotechnology, Tezpur University (A Central University), Napaam 784 028, Assam, India[3]

Abstract (250 words)

Rotaviruses (RV) cause acute severe diarrhea and are highly infectious in homologous host species. However, RV infection does not cause appreciable intestinal inflammation and homologous RV replication resists the antiviral effects of different interferon (IFN) types. In suckling mice, we found that homologous murine EW RV triggers sustained induction of IFNs, but not the amplification of interferon-stimulated genes (ISGs) or inflammatory transcripts. IFNs can trigger both apoptosis and inflammatory necroptotic cell death pathways. However, during RV infection intestinal epithelial cells (IECs) are severely impaired in the cleavage of different caspases regulating intrinsic and extrinsic cell death. Inhibition of caspase cleavage occurs in both RV-infected and -uninfected bystander IECs. In contrast, RV induces cleavage of receptor-interacting protein 1 (RIP1), a master regulator of cell death and survival decisions. Comparison of IFN-resistant (homologous) and -sensitive (heterologous) RV strains in mice demonstrates that successful RV infection restricts IFN receptor (IFNR)-amplified intestinal inflammatory cytokine secretion. LPS-mediated intestinal damage, driven by IFNR-induced inflammatory necroptosis, is also prevented during ongoing homologous RV infection. We find that the ability of RV to negate IFNR-mediated antiviral and inflammatory functions may involve a two-pronged attack. First, RV infection induces resistance to IFNAR1-directed STAT1 activation in bystander cells and inhibits IFNR-feedforward amplification. Second, ectopic stimulation of different IFNRs during RV infection results in efficient negative feedback transcription, eliminating several host innate responses to infection. Our study reveals a novel mechanism underlying the ability of homologous RV to dismantle the antiviral and inflammatory arms of several intestinal IFN types.

37 **Significance**

38 Interferons mediate distinct functions including amplification of antiviral and inflammatory
39 genes and inflammatory necroptosis of cells. Here we show that rotavirus (RV) infection
40 of small intestinal epithelial cells (IECs) subverts IFNR-mediated antiviral and
41 inflammatory functions. Although RV sensitizes both infected and uninfected bystander
42 IECs to acute necroptosis, it prevents intestinal inflammation and induces cleavage of a
43 key necroptosis regulator, RIP1K. During RV infection, uninfected bystander cells resist
44 IFN-mediated STAT1 phosphorylation and feedforward transcription is blocked. In
45 addition, ectopic stimulation of IFNRs during RV infection triggers negative-feedback
46 signaling and eliminates several host antiviral and inflammatory responses. Thus,
47 perturbation of IFNR feedback, recently linked to IFN resistance in cancer and
48 inflammatory pathologies, is also exploited by an acute viral pathogen, RV.

49 **Introduction**

50 Rotaviruses are non-enveloped segmented dsRNA viruses that cause severe
51 dehydrating diarrhea in many mammals, resulting in an estimated 200,000 human infant
52 deaths annually(1). Acute RV infection in a homologous host (the natural species in which
53 the RV strain replicates to high titer and spreads from individual to individual) is an
54 extremely efficient process; severe diarrhea can be initiated by exposure to a very small
55 infectious inoculum (2). The host innate interferon (IFN) response is a multi-pronged line
56 of defense against viral pathogens as its induction can activate hundreds of different
57 antiviral genes and trigger inflammatory signals – thus eliminating infected cells, limiting
58 the spread of virus infection to uninfected bystander cells, and shaping both the
59 magnitude and quality of subsequent adaptive immune response (3-5). The induction of
60 all three major IFN types (α/β, γ, and λ) is mounted during homologous RV infection of
61 the small bowel(6-10), but the antiviral effects of the IFN response on homologous RV
62 replication are modest at best(10). Although poorly studied, IFN-mediated inflammatory
63 responses are also likely reduced by RV infection, which is associated with only mild
64 intestinal inflammation(11, 12) compared to other acute diarrheal pathogens(13). How RV
65 efficiently subverts the ability of different IFN types to execute their antiviral and
66 inflammatory functions(14) is not well understood.

67 On the other hand, infection with *heterologous* RVs (RV not typically isolated from
68 the infected host species) generally results in severely restricted intestinal replication and
69 little or no sustained transmission to uninfected hosts(11, 15, 16). In suckling mice, the
70 intestinal replication of certain heterologous RV strains is substantially restricted (~10^4-
71 fold) but can be partially rescued by deleting IFN receptors or the downstream convergent

72 transcription factor STAT1, thus unmasking the key role of IFN in suppressing RV
73 infectivity in heterologous host species(7, 10, 11, 16). Depletion of IFNRs in suckling mice
74 can also result in an acute biliary inflammatory disease (often lethal) following infection
75 with the heterologous rhesus RV strain (RRV)(11). Thus, identifying the mechanisms by
76 which homologous RVs suppress host IFN antiviral and inflammatory responses in the
77 gut is vital for developing more effective strategies to combat RV-associated morbidities
78 and mortalities, and in understanding the pathogenic potential of naturally circulating RV
79 strains.

80 **Results**

81 **Homologous RV infection restricts intestinal IFN amplification responses.** We
82 compared the intestinal viral replication and antiviral responses between a replication-
83 restricted, IFN-sensitive simian strain (RRV), and a replication-competent, IFN-resistant
84 murine RV strain (EW)(10) at 12 and 72 hpi by qRT-PCR (Fig 1A-B). Both RV strains
85 comparably induced the three major IFN-type transcripts (IFN-α/β, IFN-γ, and IFN-λ, Fig.
86 1A) at 12 hpi. Similar *induction* of IFN pathways by both RV strains is supported at the
87 protein level by measurement of intestinal IFN-γ, which is produced in both EW and RRV
88 RV-infected mouse pups at 24 hpi (Fig. 1C). Several IFN-stimulated genes (ISGs) were
89 also transcriptionally induced at 12 hpi with similar efficiencies by both EW and RRV
90 (*IRF7*, *ISG15*, *IFIH1*, *DDX58*, *IRF9*, *IFIT2*, and *MX2*).

91 Despite inducing IFNs and various ISG transcripts with a similar or lower efficiency,
92 intestinal EW RV NSP5 transcript levels were markedly higher than RRV at 12 hpi (by
93 $>10^4$-fold, Fig. 1B). Surprisingly, at 72 hpi the induction of several IFN types and ISG
94 transcripts continued to be comparable in mice infected with either murine or simian RV

95 (Fig. 1A and Fig. S1). However, EW RV replication at 72 hpi remained substantially higher
96 than RRV RV (by ~10^4-fold, Fig. 1B and Fig. S2). The only exception to these findings
97 was *IL28A* (encoding IFN-λ2), which was significantly higher (~10 fold) in the EW RV-
98 infected pups at 72 hpi. In terms of kinetics, the induction of type I IFNs (*IFNA4* and
99 *IFNA5*) and *IRF7* transcripts by both RV strains significantly increased between 12 to 72
100 hpi while induction of IFN type II (*IFNG*) and type III (*IL28A*) declined during the infection
101 time course. Of note, the 12 hour-induction of several interferon-stimulated gene and
102 inflammatory transcriptional responses in EW RV infected pups was virtually eliminated
103 by 72 hpi (*IL6*, *CXCL10*, *ISG20*, *IFI203*, *PELI1*, *IFIH1*, *DDX58*, *IRF9*, *IFIT2*, 72 hpi, Fig.
104 1A) resembling IFN amplification responses to replication-incompetent RRV RV. Thus,
105 intestinal IFN amplification responses to EW and RRV do not mirror the marked
106 differences in actual viral replication between these two RV types. A likely explanation for
107 these results is that despite substantial continued EW RV replication in the gut and the
108 induction of IFN genes during the first 3 days of infection, homologous murine RV has
109 suppressed the amplification of intestinal ISGs and inflammatory genes by 72 hpi.
110 **Homologous rotavirus replication suppresses cleavage of several caspases in the**
111 **intestine.** The results above revealed that several IFNs continue to be transcriptionally
112 induced in a sustained manner over 72 hrs during homologous RV infection. Exposure of
113 cells to IFNs (IFN-α/β and -γ) in a sustained manner generally results in a sequential
114 cleavage of the initiator caspase 8 and the executioner caspase 3, promoting
115 apoptosis(17-20). How homologous RV contends with the potential for caspase-mediated
116 cell death while inducing different intestinal IFN types (Fig. 1A, 1C) in a sustained manner
117 is not well studied. Therefore, we next examined the expression of precursor (full-length,

118 FL) and cleaved (Cl) forms of the initiator caspase 8, which is critical for extrinsic cell
119 death(21), in murine EW RV-infected mice. Immunoblotting of small bowel IECs revealed
120 that RV infection results in a substantially lowered ratio of Cl: FL caspase 8 isoforms (2.2
121 in mock *vs.* 0.5 in RV infected at 24 hpi, but not at 3 hpi) (Fig. 2A). The defective cleavage
122 of caspase 8 (Fig.2A) would be expected to impair subsequent cleavage of the apoptotic
123 executioner caspase 3, so we next examined the status of caspase 3 during RV infection.
124 As anticipated, intestines from murine RV infected suckling mice also exhibited
125 decreased cleavage of caspase 3 (Cl.: FL ratios of 1.4 and 0.4 in mock and EW RV
126 infected, respectively, at 24 hpi but not 3hpi) (Fig. 2B). These unexpected results reveal
127 that homologous RV infection inhibits intestinal caspases at the step of their zymogen
128 activation.
129 **Cleavage of caspases 8 and 3 is inhibited in both rotavirus-infected and uninfected**
130 **bystander villous enterocytes.** Having observed that RV infection *in vivo* results in
131 impaired caspase-8 and -3 processing in IECs, we next examined whether this process
132 occurs specifically in the small intestinal villous epithelium(7). Using flow cytometry, we
133 gated live villous IECs, using a previously described combination of cell surface markers
134 (i.e. $CD45^{-}ESA^{+}CD44^{-}$)(7, 22), and then measured expression of cleaved forms of either
135 caspase 8 or caspase 3 in the RV infected and mock control pups (Fig. 2C). These
136 experiments confirmed a substantial decrease in caspase 8 and caspase 3 cleavage in
137 small intestinal villous enterocytes during RV infection (~75% decreased caspase 8 and
138 caspase 3 cleavage following infection).
139 We next examined whether caspase cleavage inhibition occurs solely in RV-infected
140 mature villous IECs at 24 hpi using a panel of antibodies to define cell type, caspase

141 activity, and the RV VP6 positivity (as a marker for RV infection status of cells) (Fig. 2D).
142 Remarkably, efficient suppression of caspase-8 cleavage occurs in both $VP6^+$ (infected),
143 and in $VP6^-$ (i.e. uninfected 'bystander') mature villous cell population. The relative ratios
144 of cells staining positive for cleaved caspase 8 in the different populations were: ~3.0
145 (mock), 0.2 (bystanders), and 0.6 (RV infected) (Fig. 2D, top panels). The efficient
146 inhibitory effect of RV infection on uninfected bystander (i.e. $VP6^-$) cells was also
147 observed following analysis of caspase 3 cleavage using a similar approach (Fig. 2D,
148 relative caspase 3 cleavage ratios were 4.0, 0.3, and 0.9 in mock, $VP6^-$ bystander, and
149 $VP6^+$ RV-infected cells, respectively; Fig. 2D, bottom panels).

150 RV inhibition of caspase 8 and 3 cleavage in both RV infected and uninfected
151 small bowel IECs would be expected to exert a significant impact on intestinal cell viability.
152 Therefore, we examined cell death in two intestinal cellular compartments. First, viability
153 analysis of total small intestinal single cell suspensions (i.e. 'bulk' level) revealed a
154 modest overall decrease in intestinal cell death during EW RV infection (this decline was
155 not statistically significant) (Fig. S3A-B). Second, a significant reduction in cell death was
156 observed by TUNEL staining of cells in the intestinal non-hematopoietic (i.e. $CD45^-$)
157 compartment, which includes both epithelial and stromal cells(7), but not hematopoietic
158 cells (Fig. S3C, $p<0.001$). Collectively, these results demonstrate that RV infection *in vivo*
159 effectively prevents caspase cleavage and suppresses intestinal cell death in both
160 infected and non-infected bystander cells.

161 In contrast to caspase 8-mediated extrinsic apoptosis, the initiator caspase 9 is
162 cleaved during intrinsic apoptosis (23). Interestingly, suckling mice infected with EW RV
163 also exhibited impaired cleavage of caspase 9 (Fig. 2E), as indicated by an accumulation

164 of intestinal FL caspase 9 at 16hpi, but not 6hpi, when compared to either RRV or mock-
165 infected controls (Fig. 2E). To examine the role of IFN in this process, we determined
166 whether caspase 9 cleavage is blocked in cultured 3T3 fibroblasts infected with the bovine
167 RV strain UK, which we previously showed triggers MAVS-dependent secretion of IFN-β
168 in this cell line(24, 25). Infection of 3T3 cells with UK RV for 9 h suppressed caspase 9
169 cleavage and mediated an accumulation of the FL-caspase 9 zymogen. In contrast,
170 increased Cl-caspase 9 and decreased FL-caspase 9 expression occurred at 16 hpi (Fig.
171 2F). These results confirmed that inhibitory effects of RV on intrinsic initiator caspase 9
172 activity do not require inhibition of IFN secretion and further indicated that caspase
173 cleavage could be regulated temporally during RV infection.

174 Kinetic regulation of caspases by RV was further examined in an intestine-derived
175 cell line by time-course analysis of caspase 8 cleavage in cultured HT-29 cells following
176 infection with porcine RV strain SB1-A, which we previously showed prevented IFN-β
177 secretion in this cell line(26). Compared to a mock-infected control, infection with SB1-A
178 RV inhibited caspase 8 cleavage starting at 4 hpi but with maximal effect occurring at 8
179 hpi (Fig. 2G). Collectively, these studies indicate that RV broadly inhibits initiatory
180 caspase cleavage events essential for either extrinsic or intrinsic cell death outcomes and
181 regulates these processes temporally during the course of infection. The results also
182 demonstrated that the RV regulatory effects on apoptotic signaling both *in vitro* (Fig. 2F-
183 G) and *in vivo* (Fig. 2A-E) occur regardless of its ability to suppress IFN induction.

184 **Several RV strains induce cleavage of the cell death regulator RIP1K.** In response
185 to sustained IFN exposure, caspase 8 cleavage results in apoptotic epithelial cell
186 shedding with typically mild inflammatory consequences(20). In contrast, in cells that are

187 defective in caspase 8 cleavage (such as IECs during EW RV infection *in vivo*, Fig. 2A-
188 C), IFN stimulation generally directs a rapid and precipitous form of cell death by
189 necroptosis that is acutely inflammatory(17, 27). Receptor interacting protein 1 kinase
190 (RIP1K) is a crucial adaptor dual-function kinase at the crossroads of a cell's decision to
191 live or die in response to either apoptotic or necroptotic stimuli(28, 29). These opposing
192 functions of RIP1K are primarily regulated by a proteolytic mechanism(30, 31). While
193 overexpression of full-length human RIP1K triggers both apoptosis and necroptosis,
194 caspase-mediated cleavage of the ~75 kDa RIP1K (p75) at multiple sites within the kinase
195 domain (KD) and interaction domain (ID) generates shorter fragments derived either from
196 the RIP1K N-terminal (51 kDa, 37 kDa, and 25 kDa) or the C-terminal (39 kDa) regions.
197 Both p51 and p39 RIP1K potently inhibit p75 RIP1K function and caspase 8 cleavage,
198 preventing apoptotic and necroptotic cell death in response to sustained inflammatory
199 stimuli(31).

200 As RV regulates caspase 8 cleavage in a temporal manner during infection (Fig. 2F-
201 G), we examined whether RIP1K cleavage is also subjected to RV regulation. HT-29 cells
202 were infected with representative RV strains differing in their modes of IFN regulation *in*
203 *vitro* (IRF3-degrading simian RRV, NF-kB inhibitory porcine SB1-A and human WI-61,
204 and NSP1-mutant simian SA11-5S RV strain that stimulates IFN-β secretion(32)) for
205 either 4 or 12 h, and then analyzed by immunoblotting using an anti-(N-terminal) RIP1K
206 antibody (Fig. 2H). When compared to mock-infected HT-29 cells, infection with the
207 different RV strains resulted in enhanced p75 RIP1K expression at 4 hpi with varying
208 efficiencies, and this increased expression was also be detected later during infection (at
209 12 hpi). In addition, RV infection also generated several shorter p51/p37/p25 RIP1K

210 cleavage fragments, and strain-specific differences were apparent in the levels of these
211 cleavage fragments. Notably, all RV strains including SA11-5S, triggered p51-RIP1K
212 cleavage starting early during infection, with the exception of the human WI-61 RV strain
213 infection where increased p51 RIP1K expression is primarily detectable by 12hpi.
214 Moreover, simian (RRV and SA11-5S) and human (WI-61) RV strains induced additional
215 cleavage of RIP1K (p37/p25 RIP1K - RRV and SA11-5S; p37 RIP1K - WI-61).
216 Interestingly, SB1-A RV induces increased expression of both the (pro-death) full-length
217 p75 RIP1K and the shorter (inhibitory) p51 RIP1K isoforms (Fig 2H, lanes 5-6). We thus
218 examined how functionally antagonistic RIP1K (p75 and p51) fragments that are
219 expressed during SB1-A infection influence cell death. We found that both cell adherence
220 and phosphatidylserine expression (a marker for apoptotic cells) at 16 hpi in SB1-A RV-
221 infected cells resembled mock-infected HT-29 cells, suggesting that increased p75 RIP1K
222 expression does not trigger cell death. In contrast, HT-29 cells treated with a cocktail of
223 tumor necrosis factor and cycloheximide exhibited substantial loss of cell adherence and
224 increased apoptotic staining (Fig. 2I). These results reveal that RIP1K accumulation and
225 its proteolysis are regulated during RV infection, and a shorter dominant-negative p51
226 regulatory RIP1K isoform is generated by many RVs early in infection that could
227 potentially impair apoptosis and necroptosis.

228 **Rotavirus restricts intestinal IFN-mediated inflammatory responses.** In addition to
229 promoting IFNR-mediated and caspase-dependent inflammatory death, different IFN
230 types can also drive the production of inflammatory cytokines by an IFNR-directed
231 positive feed-forward gene amplification process(3, 33). Therefore, we next examined
232 whether, in addition to inhibiting caspase activation *in vivo*, homologous RV infection of

233 suckling mice also suppresses the synthesis of IFNR-stimulated inflammatory target gene
234 products. To address this possibility, we used an experimental design similar to Fig. 1A
235 to measure production levels of different intestinal cytokines at 1 dpi in suckling mice
236 infected with either homologous murine (EW strain) or heterologous simian (RRV strain)
237 RVs (Fig. 3A). These studies reveal significant increases in intestinal production of a
238 variety of cytokines in response to either homologous EW and/or heterologous RRV RV
239 infection (RANTES, IP-10, IL1-A, EOTAXIN, GRO-A, MCP-3, MIP-1B, IL-4, GM-CSF, IL-
240 15, LIF; Fig. 3A). Of these, a set of cytokines (MCP-3, IL-15, LIF, IL-10, MCP-1, MIP-2α,
241 and IL-18) were increased comparably in response to either replication-competent murine
242 (EW) or replication-restricted simian (RRV) RV. In contrast, a second set of predominantly
243 pro-inflammatory cytokines (RANTES, IP-10, IL1-α, Eotaxin, GRO-α, MIP-1b, IL-6, IL-4,
244 GM-CSF, and IL-17A) were primarily induced in the heterologous simian RRV-infected
245 pups. These cytokines correlate with the poor intestinal replication of heterologous RVs
246 in mice, although whether they contribute in any manner to RRV growth restriction
247 remains to be determined. Strikingly, several differentially secreted cytokines in this set
248 are reported to be IFN-α/β, IFN-γ, and/or IFN-λ mediated effectors (i.e. RANTES(34-36),
249 IP-10(35, 37), Eotaxin(38), GRO-α(39, 40), and MIP-1b(36, 41, 42)). This suggests that
250 successful intestinal replication of homologous murine RV is accompanied by a
251 suppression of IFNR-amplified inflammatory cytokine responses(14).

252 In order to confirm whether homologous murine RV suppresses IFNR-amplified
253 inflammation, we used a suckling mouse model of endotoxemia, in which LPS-induced
254 inflammation and severe intestinal damage are reported to occur primarily through IFNR-
255 mediated inflammatory cytokine expression(43-45) and necroptotic cell death(17, 27, 46).

256 In prior work, we found that murine RV infection of the small bowel protected suckling
257 mice from endotoxin-induced mortality(8). However, whether or not EW RV replication
258 exerts a local protective effect in the LPS-challenged murine small bowel was not
259 evaluated. Here, we specifically examined if EW RV infection prevents small intestinal
260 inflammatory damage during endotoxemia (Fig 3B). Suckling mice orally infected with EW
261 RV (or mock) for 72h were systemically administered endotoxin and resulting intestinal
262 damage examined 6h later. In mock-infected mice, parenteral administration of endotoxin
263 led to severe intestinal necrosis, injury, and tissue destruction after 6h, as expected (Fig.
264 3C)(47). In contrast, suckling mice infected with murine EW RV (for 3d) prior to endotoxin
265 challenge exhibit minimal small intestinal damage (Fig. 3C). These results are consistent
266 with the conclusion that homologous RV effectively prevents IFN receptor-amplified small
267 intestinal inflammatory damage due to necroptosis or inflammatory gene expression. The
268 results also indicate, somewhat surprisingly, that efficient caspase 8 inhibition in the small
269 intestine during EW RV-infection (Fig. 2, C, D) does not sensitize mice to LPS-induced
270 inflammation.

271 **Different RV strains potentiate IFN resistance in uninfected HT-29 bystander cells.**
272 Cleaved caspase 8 is a key negative regulator of IFN (and LPS)-mediated necroptosis
273 and acute inflammation(17), and IEC-specific caspase 8 deletion results in spontaneous
274 intestinal inflammation(48), possibly triggered by constitutive tonic IFN signaling(27, 46).
275 Inhibition of caspase 8 cleavage is thus considered to be a potent priming event for acute
276 IFN-directed necroptotic inflammation in the gut(17, 21, 46). Although murine RV infection
277 reduces the cleavage of caspase 8 isoforms in both infected and bystander IECs (Fig.
278 2D), and induces various intestinal IFNs *in vivo*(7, 9) (Fig. 1A), these sequelae do not

279 translate into appreciable ISG amplification, intestinal inflammation or tissue damage
280 (Figs. 1A, 3A-C), cell death (Fig. S3), or viral growth restriction (Fig. 1B)(7, 10, 11). To
281 better understand this apparent paradox, we examined whether RV infection might block
282 IFN receptor (IFNR) signaling in both infected and bystander cells in order to effectively
283 prevent IFN effector functions. We previously reported that in cell culture, several RV
284 strains mediate efficient lysosomal degradation of endogenous IFNAR1, IFNGR1, and
285 IFNLR1 subunits in individual RV+ infected cells, but not in uninfected RV- bystander
286 cells(8).

287 We postulated that RV might employ a different strategy to also disable IFNR
288 functions in uninfected bystander cells. In previous *in vitro* studies, we showed that a
289 porcine RV strain (SB1-A) (but not several other RV strains) inhibited IFNR-mediated
290 STAT1-Y701 phosphorylation in RV- bystander cells(26), following a relatively short (i.e.
291 30-minute) stimulation with high concentrations of purified IFNβ (i.e. up to 2,000 IU/ml).
292 Here, we more extensively examined whether other RV strains might also suppress IFN
293 responsiveness in bystander cells, but with a lower efficiency than the SB1-A porcine
294 strain. This re-examination used an extended administration time for exogenous IFN
295 stimulation prior to STAT1-pY701 analysis, thus better accounting for possible lowered
296 efficiencies of IFNR inhibition by other RV strains (Fig. 4A). Human HT-29 cells were
297 infected with several RV strains (simian RRV and SA11, porcine SB1-A, bovine UK, and
298 simian SA11 mono-reassortant SOF, encoding a porcine NSP1) for 12h and cells
299 subsequently stimulated for 6h with purified IFN-β (500 IU/ml) before analysis of STAT1-
300 pY701 expression in individual RV-VP6^{+} and VP6^{-} HT-29 cells. Stimulation of mock-
301 infected cells with IFN-β activated STAT1-Y701 phosphorylation and this activation was

302 effectively inhibited by all tested RV strains in RV infected-VP6^{+} cells as we previously
303 reported(26). More importantly, STAT1-Y701 activation was also significantly inhibited in
304 RV-VP6^{-} bystander cells by the other RV strains (Fig. 4A). These results thus reveal that
305 all the RV strains tested inhibit IFN receptor signaling in bystander cellular populations *in*
306 *vitro*, although their relative efficiencies appear to vary across the strains.

307 As different IFNR types normally expressed in RV bystander cells(8) are likely to
308 be functionally impaired (Fig. 4A), we next examined how RV inhibition of IFNR-mediated
309 STAT1 phosphorylation influences downstream antiviral and inflammatory gene
310 transcriptional functions. Several ISGs and inflammatory transcripts upregulated by
311 IFNR-ligand stimulation can also be induced if cells are stimulated with intracellular
312 dsRNA, primarily through NF-kB and IRF3 signaling pathways(49). Thus, here we
313 compared the ability of RV to regulate cellular ISG and inflammatory transcriptional
314 amplification following stimulation with either exogenous IFN-β or intracellular long
315 dsRNA (Fig. 4B). Control HT-29 cells stimulated with IFN-β or dsRNA triggered both
316 overlapping (*TNF, TNFAIP3, HERC5, IFI6, IFIT3, IFIT1, IFNB1, RSAD2*) and unique
317 (*TLR2, IL26, IL21, SERPING* by IFN-β; *IL29, IFNG* by dsRNA only) sets of transcriptional
318 responses. Regardless of how transcriptional stimulation was carried out, RV infection
319 effectively prevented further transcriptional upregulation of *HERC5, IFNG, IL22, IL21,*
320 *IFI6, IFIT1, IFIT3*, and *RSAD2*. In contrast, we identified a set of pro-inflammatory
321 transcripts that was specifically blocked by RV in response to exogenous IFN-β, but not
322 to intracellular dsRNA (*TLR2, IL26, TNF, IRF8, TNFAIP3, IL29, IL1B)*. Among the
323 transcripts measured, only *SERPING* was efficiently induced by IFNAR1 stimulation
324 during RV infection, though with a lowered efficiency than in uninfected HT-29 cells. The

325 stimulus-specific RV inhibition of transcription was not due to RV replication sensitivity,
326 since it was unaltered under either the IFN-β or dsRNA stimulation conditions used (Fig.
327 4C). In addition, the induction of certain transcripts was specifically repressed by ectopic
328 IFNAR1 stimulation during RV infection (*HERC5, IFNG,* and *IL22,* statistically significant
329 $p<0.01$*; IRF8, IL29,* and *IL1B,* not statistically significant). These results demonstrate that
330 RV effectively inhibits IFN-β-receptor mediated transcription of selected ISGs and
331 inflammatory genes. In addition, they indicate that ectopic IFNAR1 stimulation during the
332 course of RV infection can elicit negative feedback inhibition of transcription (Fig. 4B, 4D).
333 Such feedback-based regulation(50) is likely to be particularly relevant to antiviral and
334 inflammatory functions in uninfected RV- bystander cells that, unlike a RV+ infected cell,
335 express IFNRs (8) (Fig. 4D).

336 **Murine RV infection re-purposes IFNR-directed intestinal antiviral and**
337 **inflammatory signaling.** The stimulation of IFNGR1 and IFNAR1 is reported to suppress
338 STAT1 via negative feedback signaling under certain conditions, fostering IFN-resistance
339 in the context of cancer and chronic viral infection(33, 50). We examined whether
340 intestinal IFNR-mediated transcription is altered by homologous RV *in vivo* to suppress
341 IFN antiviral and inflammatory signaling (Fig. 1A and 3A). Following infection of suckling
342 mice with murine EW RV for 12h, we parenterally administered purified IFN-γ (or PBS),
343 and collected small intestines after an additional 12h for transcriptional analysis (Fig. 5A).
344 In mock-infected control pups, IFN-γ stimulation upregulated several intestinal transcripts
345 (*STAT1, ISG15, IFI204, IL10RA, IL1RN,* statistically significant*; S100A8, BIRC5, REG3G,*
346 not significant; Figs. 5B-5D). In contrast, transcription of *CCL5* was significantly repressed
347 by ectopic IFNGR1 stimulation. Similar transcriptional responses are also upregulated by

348 EW RV infection, but with magnitudes significantly larger than obtained by IFN-γ
349 stimulation alone. A set of antiviral (*DHX58, DDX58, MX2*) and inflammatory (*TRAIL,*
350 *NOS2, CXCL10*) transcripts was significantly upregulated by RV, but not by IFN-γ
351 stimulation. Remarkably, ectopic stimulation of the IFNGR1 in EW RV-infected mice
352 either significantly suppressed (*STAT1, ISG15, TRAIL,* and *CXCL10*) or completely
353 eliminated (*DHX58, DDX58, MX2, CCL5,* and *NOS2*) these intestinal antiviral and
354 inflammatory responses (Fig 5B-C). In contrast, IFN-γ stimulated, EW RV-infected pups
355 upregulated anti-inflammatory and proliferative gene transcription (*S100A8, BIRC5,*
356 *ARG2, REG3G, MKI67,* and *IL1RN*) (Fig. 5D). These transcripts were not significantly
357 induced by either IFN-γ stimulation or by EW RV-infection alone, and synergistically
358 increased when IFNGR1 stimulation was carried out during EW RV infection. To ascertain
359 whether the effects of IFN stimulation in EW RV-infected pups could be explained by
360 altered RV replication levels, we measured intestinal RV RNA by qRT-PCR. The results
361 demonstrate that EW RV replication was not significantly altered following IFN-γ
362 stimulation (Fig. 5E). These findings suggest that during homologous RV infection,
363 intestinal IFNR function can be diverted towards suppressing antiviral and inflammatory
364 responses and promoting an anti-inflammatory program, revealing a potential
365 mechanism by which uninfected RV bystander cells resist the antiviral and inflammatory
366 effects of IFN secreted by IEC and enteric hematopoietic cells(7, 51).

367 **Discussion**

368 Interferons are pleiotropic innate immune effectors that constitute a primary line of
369 defense against viral pathogens. By signaling through their cognate receptors, different
370 IFN types potentiate the expression of numerous and multi-functional antiviral and

371 inflammatory genes(4, 5). In addition, IFNR stimulation can also induce apoptotic and
372 necroptotic forms of cell death(17-19, 46), possibly to limit viral replication and spread. In
373 its homologous host species, RV replication is only marginally restricted by the induction
374 of different IFNs and robust viral replication is not associated with substantial
375 inflammation(7, 8, 10, 11, 16). However, heterologous RV replication is highly restricted
376 by each of the three major IFN types(10). How homologous RVs manage to avoid the
377 antiviral and inflammatory actions of IFNs is still not fully understood.

378 We found that in suckling mice, mucosal innate immune transcriptional responses
379 to the virulent and highly infectious murine EW RV strain closely resembled those to a
380 replication-restricted heterologous simian strain (Fig.1A). The similarity in innate
381 responses - including IFN type transcription, IFN-γ production, and amplification of ISGs
382 or inflammatory gene transcripts over time (Fig. 1C) - did not correlate well with the very
383 different replication levels of the EW vs. RRV (approximately 10,000-fold difference, Fig.
384 1B). Different IFN type transcripts remained significantly elevated at 72 hpi in EW RV-
385 infected pups, indicative of a sustained innate immune response to ongoing RV
386 replication. However, we did not observe amplification of several ISGs (i.e. *ISG15, ISG20,*
387 *IFI203, IFIH1, DDX58, IRF9*, and *MX2* (Fig. 1A) during the later stages of EW infection.
388 These results indicated that although homologous RV replication and IFN induction occur
389 in a sustained manner during infection, this does not effectively lead to sustained
390 amplification of multiple antiviral and inflammatory genes.

391 In response to sustained IFN exposure, apoptosis can occur via proteolytic
392 activation of the initiator caspase 8(19, 20). IFN-stimulated apoptosis is a relatively slow
393 process, likely mediated by IFN-stimulated expression of intermediary apoptotic ligands

394 (e.g., FasL and TRAIL)(18-20), and typically has mild inflammatory consequences. In
395 addition to triggering apoptosis, proteolytic cleavage of pro-caspase 8 can suppress
396 necroptosis - a more inflammatory form of cell death(17, 52). Necroptosis is rapidly
397 activated when cells are deficient for caspase 8, or in the presence of caspase inhibitors,
398 following exposure to inflammatory ligands like TNF-α or FasL(21). Ligand stimulation of
399 the IFN-α/β and -γ receptors can also precipitate rapid cellular necroptosis, leading to
400 acute inflammation(17, 21). This process is mediated by currently unknown but critical
401 IFNR-dependent effectors (termed constitutively IFN-regulated effectors of necroptosis,
402 CIRENs)(46). In addition, IFNs can amplify the expression of inflammatory cytokine genes
403 encoding IFN-sensitive response promoter elements. Both IFN-mediated necroptosis and
404 inflammatory gene expression require an intact IFNR signaling pathway and are critical
405 mediators of acute intestinal inflammation in response to endotoxin(17, 21, 43, 46, 53).
406 Of note, before this set of experiments, the regulated cell death and inflammatory arms
407 of IFN receptor signaling had not been well studied in the context of RV infection.

408 Our results suggest that homologous RV infection initiates a two-pronged set of
409 events to subvert and delay IFN-mediated cell death functions and potentially allow more
410 time for RV replication within IECs. An estimated 1400 cells/villous/day are normally shed
411 to maintain intestinal homeostasis in an adult mouse(54). We found that a key step in
412 epithelial cell turnover, the cleavage of caspases 8 and 3, was significantly inhibited
413 during homologous RV infection in both virus-infected and uninfected bystander mature
414 villous IECs (Fig. 2, S3). This blockage of caspase activation may serve to prevent or
415 diminish IFN-accelerated apoptosis and thus enhance viral replication and spread to
416 uninfected IECs. The inhibition of caspase 3 activity could itself result from RV-inhibited

417 cleavage of the upstream initiator caspase 8 (Fig. 2A, 2C-D), which mediates caspase 3
418 activation by the extrinsic death pathway and is inhibited in both RV-infected and
419 bystander IECs (Fig. 2D). In addition, homologous murine RV also hampers homeostatic
420 cleavage of another initiator caspase (caspase 9) that is crucial for executing intrinsic cell
421 death pathways. The ability of RV to regulate multiple types of caspases *in vivo* is novel
422 and, to the best of our knowledge, represents an ingenious viral strategy to broadly
423 regulate and delay several effectors of intestinal cell death. The inhibition of caspase
424 cleavage also occurs during RV infection *in vitro* and is temporally regulated (Fig. 2F, G).
425 The mechanism by which cleavage of the different types of caspases is regulated
426 by RV is presently unknown. Nevertheless, analysis of a key caspase 8-regulated
427 signaling effector, RIP1K(28, 30, 53), in RV-infected HT-29 cells provides possible insight
428 into underlying mechanisms. Specifically, we found that *in vitro* different strains of RV
429 promoted the cleavage of full-length p75 RIP1K into shorter fragments (i.e. p51, p37, and
430 p25) (Fig. 2H). The cleavage of RIP1K into the p51 fragment is caspase 8-mediated and
431 generates a negative regulator that can prevent apoptotic and necroptotic cell death in
432 cells constantly exposed to inflammatory stimuli(31). In contrast to the regulation of RIP1K
433 by caspase 8, under certain conditions (e.g. ER stress) RIP1K is required for proper
434 caspase 8 cleavage and apoptosis(55). This suggests the existence of a regulatory
435 feedback of RIP1K on caspase 8 activity. One possible explanation of our findings could
436 be that one or more RIP1K cleavage products generated early during RV infection (Fig.
437 2H) regulate caspase 8 cleavage and cell death during ER stress conditions that occur
438 later in RV infection(56-59). Time-course analyses of caspase 8 and RIP1K cleavage
439 during RV infection (Fig 2G-H) indicated that both these processes are impaired

440 temporally, but do not mediate appreciable levels of cell death or apoptotic markers even
441 at relatively late times of infection (Fig. 2I). It will be interesting to determine whether these
442 RIP1K regulatory processes occur in RV bystander cells and to identify the viral and host
443 effectors involved.

444 Regardless of the exact underlying mechanisms, impaired caspase 8 cleavage in
445 both RV infected and bystander IECs (Fig. 2D) creates a potentially problematic situation
446 in the intestinal epithelium(21). IEC-specific caspase 8 deletion by itself is sufficient to
447 trigger spontaneous intestinal inflammatory lesions, resulting in terminal ileitis and
448 colitis(48, 60). As noted above, caspase 8 cleavage inhibition is also a key priming event
449 that triggers IFN receptor-mediated necroptosis, acute inflammation, and endotoxin-
450 induced tissue damage(17-19, 27, 46, 53, 60). Paradoxically, we found that murine EW
451 RV infection significantly protected suckling mice from subsequent lethal endotoxemia
452 (100% vs. 0% survival, at 24h post-endotoxin exposure)(8). Since endotoxin-mediated
453 damage is potentiated by IFN receptor-stimulated inflammatory gene expression(44) and
454 necroptotic cell death(27), it seemed plausible to postulate that homologous RV infection
455 locally represses IFN-mediated inflammatory functions in the small intestine. Our
456 histopathologic findings (Fig. 3C) confirm that, at the local small bowel level, EW RV-
457 infected murine pups are substantially protected from severe inflammatory damage due
458 to exogenous endotoxin exposure. An interesting question raised by these findings, which
459 we are currently examining, is whether similar protective effects of RV on inflammation
460 can occur at extra-intestinal sites. Homologous RV infection also blocked the IFN
461 receptor-stimulated inflammatory gene expression program, as indicated by the finding
462 that intestinal secretion of several IFN-stimulated inflammatory cytokines (RANTES(34-

463 36), IP-10(35, 37), Eotaxin(38), GRO-α(39, 40), MIP-1b(36, 41, 42)) were all significantly
464 lower in the murine RV-infected pups compared to a replication-restricted heterologous
465 simian RV, despite substantially higher replication levels of the murine strain (Fig. 3A).

466 Rotavirus efficiently degrades multiple IFNR types in infected cells(8), which is
467 predicted to directly limit both IFN-mediated inflammatory cell death and gene
468 amplification by depleting surface IFNR expression. The RV protein(s) that mediate IFNR
469 degradation have not been identified, although the RV-encoded non-structural protein
470 NSP1 would seem to be the most likely candidate due to its ability to inhibit STAT1
471 signaling and cause the degradation of both IRF3 and bTrCP(26, 32, 61). In this study we
472 examined whether IFNR function in bystander cells was also inhibited by RV. We
473 previously reported that a porcine RV strain (SB1-A) prevents STAT1-Y701
474 phosphorylation in uninfected RV- bystander HT-29 cells following *a relatively short (i.e.*
475 *30 min) ectopic IFN exposure*(26). Whether non-porcine RVs also prevent IFN-mediated
476 signaling in bystander cells was not explored further using altered IFN stimulation
477 conditions. Here, using a more prolonged IFN stimulation (i.e. 6 h) combined with FACS
478 analysis, we demonstrate that several non-porcine RV strains, shown previously to
479 mediate IFNR degradation in infected cells, also induce effective resistance to IFN-
480 directed STAT1-pY701 in bystander cells (Fig. 4A).

481 The ability of various RV strains to block IFN signaling in bystander cells is a
482 second prong of the viral strategy to subvert antiviral and inflammatory functions mediated
483 through the IFNRs. The effector functions of different IFNs are precisely titrated by a
484 sensitive receptor-centered negative-feedback modulating mechanism(62-64), ensuring
485 that excessive inflammatory damage to the host does not occur by uncontrolled feed-

486 forward IFNR signaling. Dysregulation of this equilibrium can lead to either IFN resistance
487 exemplified by cancer cells(65), or to acute inflammatory pathologies(66),such as sepsis.
488 Previously, we demonstrated that parenteral IFNγ administration results in efficient
489 STAT1-pY701 activation in small intestinal epithelial cells, a process that is significantly
490 suppressed during homologous EW RV infection in suckling mice(8). A similar
491 perturbation of IFNR-mediated STAT1 activation by murine EW RV occurred if purified
492 IFN-β or IFN-λ was used to stimulate their cognate receptors(8). Earlier studies also
493 identified a STAT1-independent pathway that regulates IFNγ-stimulated gene
494 expression(67-70). More recently, the production of inflammatory cytokines in response
495 to toll-like receptor (TLR) stimulation was significantly suppressed by ectopic IFNγ and
496 IFNβ stimulation of STAT1-null cells, by re-purposing IFNGR1 and IFNAR1 signaling
497 toward feedback inhibition(50). In this study, we examined whether such alternate IFNR
498 signaling could also be usurped by RV to broadly suppress innate antiviral and
499 inflammatory responses.
500 Several transcripts upregulated during the IFNR feed-forward amplification phase
501 can also be efficiently induced by intracellular dsRNA through signal transduction of
502 different pattern recognition receptors, including the RIG-I-like-receptors (RLRs), toll-like-
503 receptors (TLRs), and the dsRNA-dependent protein kinase (PKR)(3). We therefore
504 compared the ability of dsRNA- and IFNβ-stimulation to upregulate antiviral and
505 inflammatory gene expression during RV infection of HT-29 cells (Fig. 4B). As RV^+
506 infected HT-29 cells are efficiently depleted of different IFNRs, an assumption in our
507 experiment was that IFNβ-stimulated transcription occurs via the IFNRs expressed on
508 uninfected RV- bystanders, although we did not directly demonstrate this. The results

509 clearly indicated an efficient inhibition of feed-forward transcriptional responses to IFNR
510 stimulation by RV, when compared to intracellular dsRNA stimulation (Fig. 4B).
511 Interestingly, IFNβ stimulation during the course of RV infection repressed *HERC5*, *IFNG*,
512 *IL22, IRF8, IL29,* and *IL1B* transcription, suggesting that IFNAR1 stimulation (presumably
513 of uninfected RV- bystander cells) might also trigger an inhibitory feed-back transcription
514 mode (Fig. 4C).

515 In subsequent experiments, we quantified intestinal IFNR-stimulated transcription
516 during homologous EW RV (or mock) infection by ectopically stimulating the IFNGR1 in
517 suckling mice (Fig. 5A). These results demonstrated that, in contrast to a feed-forward
518 'priming' transcriptional mode in mock controls, IFNγ stimulation during EW RV infection
519 potentiates decreased ISG and inflammatory transcripts (*STAT1, ISG15, IFI204, DHX58,*
520 *DDX58, MX2, CCL5, TRAIL, NOS2,* and *CXCL10*) (Fig. 5B-C). In addition, we found that
521 ectopic IFNGR1 stimulation during EW RV infection (but not IFNγ stimulation or EW RV
522 alone) synergistically increases the transcription of anti-inflammatory transcripts (Fig.
523 5D). Interestingly, several of these upregulated genes (i.e. *S100A8, BIRC5, ARG2,*
524 *REG3G,* and *MKI67*) are targets of the STAT3 signaling pathway, whose activation is
525 reported to suppress STAT1-mediated inflammatory and antiviral programs due to IFNR
526 stimulation(33, 68-70). We are currently examining whether STAT3 activation occurs
527 during RV infection and mediates IFNR feedback signaling.

528 Collectively, our findings demonstrate that RV effectively reprograms IFNR-relayed
529 transcription towards suppressing antiviral and inflammatory amplification (Fig. 3, 4, 5), a
530 process whose efficiency is expected to be enhanced by IFNs generated in the local
531 intestinal milieu during enteric RV infection (Fig. 1). The ability of RV infection to

532 reprogram IFNR transcriptional function identifies an underlying mechanism by which
533 other IFNR functions, such as caspase cleavage-mediated cell death could also be
534 controlled by RV.

535 **ACKNOWLEDGEMENT**

536 This work was supported by grants 1RO1 AI021362, R56 AI125249, and 1RO1
537 AI1125249 from the National Institutes of Health, and 1IO 1BX000158-01A1 from the
538 Veterans Affairs. We thank Catherine Cruz for carrying out initial studies and helpful
539 scientific discussions during the study.

540

541

542 **FIGURE LEGENDS**

543 **Figure 1. Effects of replication-competent (homologous, murine) and replication-**
544 **restricted (heterologous, simian) RV strains on intestinal interferon-stimulated**
545 **gene (ISG) and inflammatory transcriptional responses.** (A-B) Transcriptional
546 analysis of intestinal transcriptional responses to murine EW and simian RRV RV strains.
547 Three- to five-day old suckling mice (N=4 per group) were infected with murine EW or
548 simian RRV RV strains (or mock), and at 12 h or 72 h small intestines were collected for
549 transcriptional analysis of host (A) and RV (B) genes. (C) Intestinal secretion of IFN-γ was
550 measured by Luminex following RV infection at 24 hpi as in (A) (N=3 samples per group,
551 each sample pooled from 3 pups; ND, not detected).

552

553 **Figure 2. Rotavirus suppresses the cleavage of multiple caspases and promotes**
554 **the cleavage of receptor-interacting protein 1 kinase (RIP1K).** (A-B) Analysis of

555 caspase 8 and caspase 3 expression. Mouse pups were orally inoculated with EW (R) or
556 mock-inoculated (M). At 3 and 24 hpi, bulk intestinal cells were harvested from whole
557 small intestinal tissues and processed for SDS-PAGE. Gels were analyzed by western
558 blot for precursor (FL) and cleaved (Cl.) isoforms of either caspase 8 (A) or caspase 3
559 (B), and other proteins. The normalized ratios of Cl. to FL caspases determined by
560 densitometry are indicated below individual panels. (C) FACS analysis of caspase 8 and
561 caspase 3 cleavage. Summary of flow cytometry analysis of $CD45^{-}CD44^{-}ESA^{+}$ IECs
562 following intracellular staining for KI67, and either cleaved caspase 8 or cleaved caspase
563 3, from EW RV infected or control pups at 24 hpi. (D) The percentage of IECs ($CD45^{-}$
564 $CD44^{-}ESA^{+}$) displaying cleaved caspase 8 or cleaved caspase 3 in mock and EW-
565 infected mice at 24 hpi averaged from three experiments; error bars represent the
566 standard errors of the means. (E) Intracellular staining for RV structural protein (VP6) and
567 either cleaved caspase 8 (top panel) or cleaved caspase 3 (bottom panel) in $CD45^{-}CD44^{-}$
568 ESA^{+} IECs following EW RV or mock infection at 24 hpi. (F) Immunoblotting analysis of
569 small intestinal tissue from mouse pups infected with EW, RRV, or mock, and harvested
570 at the indicated times. (G) Analysis of caspase 9 cleavage in cultured NIH 3T3 fibroblasts
571 infected with an IFN-stimulatory RV strain, UK. 3T3 cells were infected with bovine UK
572 RV (or mock) for the times indicated and then analyzed by immunoblotting. Numbers
573 below blots indicate normalized ratios of Cl. to FL caspase 9. (H) Human HT-29 IECs
574 were infected with porcine SB1-A RV (or mock) for the times indicated and analyzed by
575 immunoblotting. Numbers below blots indicate normalized ratios of Cl. to FL caspase 8.
576 (I) HT-29 cells infected with the RV strains indicated were analyzed for RIP1K, RIP3K,
577 and VP6 at either 4 or 12 hpi by immunoblotting. (J) HT-29 cells were infected with SB1-

578 A RV (or mock), or treated with TNF-alpha (10ng/ml) and cycloheximide (10μg/ml) for 4
579 h, and then analyzed for cell adherence or phosphatidyl serine marker expression. Data
580 shown is representative of two or more independent experiments.
581
582 **Figure 3. Effects of replication-competent (homologous, murine) and replication-**
583 **restricted (heterologous, simian) RV strains on intestinal cytokine production. (**A)
584 Secretion of intestinal cytokines during RV infection of suckling mice. Suckling mice were
585 infected as in Figure 1, and small intestinal homogenates were analyzed at 24 hpi for the
586 indicated cytokine protein levels (N=3 samples per group, each sample pooled from 3
587 pups and measured in duplicate). (B) Schematic of reported endotoxin-mediated
588 inflammation that is IFNR-stimulated and negatively regulated by cleaved caspase 8. (C)
589 Effect of homologous RV infection in suckling mice on endotoxin-mediated intestinal
590 damage. Suckling mice were mock- or EW RV-infected and 3 d later were parenterally
591 administered purified endotoxin (15μg/pup) for 6 h before harvesting small intestines for
592 histological examination by hematoxylin and eosin staining. Data shown is representative
593 of 2 pups.
594
595 **Figure 4. Rotavirus potentiates resistance to IFN receptor-mediated STAT1**
596 **activation and transcriptional function. (**A) Different RV strains trigger resistance to
597 IFN-mediated STAT1-Y701 phosphorylation in bystander cells. HT-29 cells were infected
598 with the RV strains indicated and 12 h later, stimulated with 500 IU/ml of purified IFNβ for
599 6 h before FACS analysis. Numbers in red indicate fold increases in STAT1-pY701
600 following IFN stimulation in RV VP6+ (infected) and VP6- (bystander) populations. Data

601 is representative of two independent experiments. (B-C) Effect of RV infection on dsRNA-
602 and IFN receptor-mediated transcriptional activity. Schematic at the top depicts the
603 experimental approach used. HT-29 cells were infected with RV (RRV strain, at an MOI
604 of ~0.5) or mock-infected and at 6 hpi, cells were either transfected with 2μg of purified
605 dsRNA or were stimulated with 500 IU/ml of purified IFNβ. At 12 hpi cells were analyzed
606 by qRT-PCR for expression of host (B) and RV (C) transcripts. Data represents two
607 independent experiments. (D) Schematic summarizing differential inhibition of dsRNA-
608 and IFN receptor-stimulated transcription by RV. Dashed red line indicates possible
609 negative feedback signaling upon ectopic IFNR stimulation during RV infection, solid red
610 lines indicate RV inhibition of IFNRs by receptor degradation (in RV-infected cells(8)) and
611 by blockage of IFNR-mediated STAT1 activation and transcription (in RV bystanders).
612
613 **Figure 5. Rotavirus infection re-purposes IFN receptor-directed intestinal and**
614 **inflammatory signaling.** (A) Schematic of the experimental approach used. (B-E)
615 Transcriptional analysis of different assigned categories of intestinal transcripts following
616 ectopic stimulation of the type II IFN receptor. Mice were infected with EW RV (or mock)
617 (N=3-5 pups per group) and at 12 hpi were administered purified murine IFNγ (1μg/pup,
618 or PBS, i.p.). Twelve hours later mice were sacrificed, and small intestinal RNA was
619 analyzed by qRT-PCR for different host (B-D) or RV NSP5 gene (E) transcripts.
620
621

622 **MATERIALS AND METHODS**

623 **Viruses and reagents.** The tissue culture-adapted RV strains (simian RRV, SA11-4F,
624 SA11-5S, human WI-61, porcine SB1-A, bovine UK) were propagated in African green
625 monkey kidney cells (MA104) as previously described (71). Virus titers were determined
626 by plaque assays in MA104 cells. HT-29 cells were plated in 6-well or 24-well cluster
627 plates and completely confluent monolayers were infected 2-3d later as described. The
628 non-tissue culture-adapted murine EW RV strain was prepared as an intestinal
629 homogenate from RV-infected BALB/C suckling mice. The diarrheal dose (DD_{50}) was
630 determined as previously described (16). Human intestinal epithelial HT29 and embryonic
631 kidney HEK293 cells were purchased from the American Type Culture Collection (ATCC)
632 and maintained in Advanced D-MEM Ham's F12 (Cellgro) or D-MEM medium (D-MEM,
633 Cellgro) containing 10% fetal calf serum (Invitrogen) supplemented with non-essential
634 amino acids, glutamine, penicillin, and streptomycin, respectively. Purified human IFN-β
635 (PBL), human IFN-λ (PBL), and human IFN-γ (Millipore) were used for stimulation of cells.
636 Purified carrier-free human IFN-β (PBL), murine IFN-γ, human TNF-α (R&D System,
637 Minneapolis, MN), LPS (Sigma) were used. Cycloheximide (Sigma) and high-molecular
638 weight LyoVec poly(I:C) (Invivogen) were used at 10 µg/mL and 2.5 µg/mL, respectively.

639 **Mouse infection and tissue harvest.** All mice were housed in the VA Palo Alto Health
640 Care System (VAPAHCS) Veterinary Medicine Unit and all experimentation followed
641 VAPAHCS Institutional Animal Care and Use Committee approved protocols. 3-5 day
642 old Sv129 pups were infected via oral gavage with 10^4 DD_{50} of murine EW RV, 10^7 PFU
643 of the simian RRV, or mock infected with 1X M199 media (Gibco) as described (16). (16).
644 At the indicated time-points, the small intestines were removed. Sections were stored at

645 -80 °C or fixed in 4% paraformaldehyde for processing and subsequent analyses. The
646 protocol for IEC isolation, as previously described (72), was slightly modified. Briefly, the
647 intestines were removed and opened longitudinally in RPMI media supplemented with
648 penicillin, streptomycin, and L-glutamine (Gibco). The intestines were washed, cut into
649 smaller pieces, and placed in 1X PBS containing 5 mM EDTA and 5 mM DTT (Sigma-
650 Aldrich). Tissues from 3-4 pups (per infection group) were pooled at this point. The tissues
651 were then placed on a shaker for 10 minutes at room temperature. Released cells were
652 subsequently filtered through a 100-µm mesh filter into fresh RPMI FBS media (RPMI
653 supplemented with 10% fetal bovine serum, penicillin, streptomycin, and L-glutamine) and
654 immediately placed on ice. The remaining tissues were then incubated with fresh RPMI
655 FBS media and rocked for an additional 10 minutes, followed by a final wash in RPMI
656 FBS media for an hour. Cells were filtered, washed, and resuspended in PBS for further
657 analyses.
658 **Mouse stimulation and Luminex assays:** To ectopically stimulate IFNGR1, suckling
659 mice infected with 10^4 DD_{50} of murine EW RV (or mock-infected) were intraperitoneally
660 administered purified murine IFN-γ (1μg IFN-γ per pup) or IFN- λ2 at 12 hpi and sacrificed
661 12 h later for analysis of transcripts by qRT-PCR. For endotoxin stimulation, 3-5 day old
662 129sv mice were orally inoculated by gavage with 10^4 DD_{50} of murine RV-EW. At 3 dpi,
663 mice were intraperitoneally injected with PBS or purified LPS (Sigma, 10 mg/kg body
664 weight) and sacrificed 6 h later for analysis of paraformaldehyde-fixed and paraffin
665 embedded tissue sections by hematoxylin and eosin staining. For measurement of
666 intestinal cytokines, mouse intestines were harvested and weighed pooled tissues were
667 homogenized in ice-cold PBS containing a cocktail of protease and phosphatase

668 inhibitors (Sigma) using a handheld micropestle (Thermo Fisher). Lysates were clarified
669 by two sequential rounds of centrifugation at 10,000X G for 10 min, and analyzed for
670 cytokine levels at the Human Immune Monitoring Center at Stanford University. Mouse
671 38-plex kits were purchased from eBiosciences/Affymetrix and used according to the
672 manufacturer's recommendations. Plates were read using a Luminex 200 instrument with
673 a lower bound of 50 beads per sample per cytokine. Custom assay Control beads by
674 Radix Biosolutions are added to all wells.

675 **Western blot analysis.** Preparation of cell lysates and immunoblotting in vitro was
676 performed as described. For mouse samples, EDTA/DTT-treated IECs were lysed in
677 radioimmunoprecipitation assay buffer (RIPA) supplemented with protease and
678 phosphatase inhibitors (Roche). Equal volumes of 2X Laemmli buffer (Sigma-Aldrich)
679 were added to each sample and analyzed by immunoblotting. Blots were probed with the
680 following primary antibodies: anti-caspase 3, anti-caspase 8, anti-caspase 9, anti-cleaved
681 caspase 3, anti-cleaved caspase 8, anti-cleaved caspase 7, anti-PARP, anti-GAPDH,
682 anti-survivin, anti-STAT-3, anti-p-STAT-3 (Y705) (all from Cell Signaling Technologies)
683 and an anti-RV capsid antibody (from Santa Cruz Biotechnologies). The blots were
684 subsequently incubated with either anti-rabbit or anti-mouse secondary antibodies
685 conjugated to horseradish peroxidase (HRP), incubated with ECL Detection reagent, and
686 exposed to film (GE Healthcare). All densitometry quantifications of protein blots were
687 analyzed using ImageJ software analysis and normalized to GAPDH protein bands.

688 **Transcriptional analysis.** For *in vivo* analysis of transcripts, mice were sacrificed and
689 sections of the small intestine were collected on ice in Trizol (Life Technologies). For *in*
690 *vitro* studies, cells were first washed in PBS and then lysed in Trizol. Total RNA was

691 extracted following the manufacturer's instructions and subjected to DNAse digestion
692 before use in qRT-PCR. Synthesis of cDNA and subsequent microfluidics PCR on the
693 Fluidigm platform was done as described earlier (73). Serial 10-fold dilutions of mouse or
694 human reference RNA (Agilent) were run in duplicate for each PCR run.

695 **Flow cytometry analysis.** For flow cytometry analysis of caspase expression and cell
696 viability *in vivo*, mouse intestines were harvested as described above and equivalent
697 numbers of EDTA/DTT-treated IECs were stained for cell viability using Invitrogen's
698 LIVE/DEAD Fixable Aqua Dead Cell Stain Kit following the manufacturer's protocol. Cells
699 were blocked with purified rat anti-mouse CD16/CD32 Fc Block (BD Biosciences) and
700 stained for the following murine surface markers: anti- CD45 (clone 30-F11) v450 (BD
701 Biosciences), anti- CD326 (Ep-CAM/ESA, clone G8.8) PE (Biolegend), and anti- CD44
702 (clone IM7) PerCP/Cy5.5 (Biolegend) as described earlier (7). Cells were then fixed and
703 permeabilized with BD Cytofix/Cytoperm Fixation/ Permeabilization buffer according to
704 the manufacture's protocol and subsequently used for intracellular protein staining. To
705 perform intracellular protein staining, cells were blocked with BD Fc Block and incubated
706 with unconjugated antibodies to cleaved caspase 8 (Cell Signaling Technologies) or
707 cleaved caspase 3 (Cell Signaling Technologies) along with conjugated antibodies to RV
708 VP6 (1E11-Texas Red) and Ki67 (Alexa Fluor 647, BD Biosciences). Subsequently, cells
709 were incubated with a secondary goat anti-rabbit-Alexa Fluor 488 antibody (Molecular
710 Probes) for detection of cleaved caspases. All data was acquired using a LSRII (BD
711 Biosciences) and analyzed with FlowJo software (Treestar Inc). Staining and flow
712 cytometry analysis of HT-29 cells was performed as described.

713 **TUNEL and apoptosis assays.** For TUNEL, following surface staining of intestinal
714 epithelial cells (as described above), cells were fixed and permeabilized for subsequent
715 determination of DNA fragmentation using Roche's In Situ Cell Death Detection Kit-
716 Fluorescein (following the manufacturer's protocol). Briefly, cells were fixed in 2% PFA
717 and permeabilized in 0.1% Triton X-100 in 0.1% sodium citrate buffer and incubated with
718 the terminal deoxynucleotidyl transferase (TdT), along with fluorescein-dUTP labeling
719 solution for 1 hour at 37 °C. As a positive control, permeabilized IECs were treated with
720 DNase I (Ambion) for 30 min at 37 °C (to induce DNA fragmentation) prior to the TUNEL
721 reaction. An additional negative control (labeling reactions carried out without TdT
722 enzyme) was also included. Incorporation of labeled dUTP was analyzed on a LSRII flow
723 cytometer. To assay apoptosis marker expression in HT-29 cells, cells were washed with
724 PBS, stained with Apopxin Green (1:100 dilution, Abcam) at room temperature for 10
725 minutes, and washed before examination by fluorescence microscopy.
726 **Statistical analysis.** Analysis of variance (ANOVA) and 2-tailed student's t-tests were
727 performed using GraphPad InSTAT software. Figure legends indicate the specific tests
728 used and P values <0.05 were considered significant. All error bars represent the
729 standard error of the mean.
730

731 **REFERENCES**

732 1. Kirkwood CD, Ma LF, Carey ME, & Steele AD (2017) The rotavirus vaccine development
733 pipeline. *Vaccine*.
734 2. Broome RL, Vo PT, Ward RL, Clark HF, & Greenberg HB (1993) Murine rotavirus genes
735 encoding outer capsid proteins VP4 and VP7 are not major determinants of host range
736 restriction and virulence. *J Virol* 67(5):2448-2455.
737 3. Talemi SR & Hofer T (2018) Antiviral interferon response at single-cell resolution. *Immunol*
738 *Rev* 285(1):72-80.
739 4. Cicchese JM*, et al.* (2018) Dynamic balance of pro- and anti-inflammatory signals controls
740 disease and limits pathology. *Immunol Rev* 285(1):147-167.
741 5. Yan N & Chen ZJ (2012) Intrinsic antiviral immunity. *Nat Immunol* 13(3):214-222.
742 6. De Boissieu D, Lebon P, Badoual J, Bompard Y, & Dupont C (1993) Rotavirus induces alpha-
743 interferon release in children with gastroenteritis. *J Pediatr Gastroenterol Nutr* 16(1):29-
744 32.
745 7. Sen A*, et al.* (2012) Innate immune response to homologous rotavirus infection in the
746 small intestinal villous epithelium at single-cell resolution. *Proc Natl Acad Sci U S A*
747 109(50):20667-20672.
748 8. Sen A, Sharma A, & Greenberg HB (2017) Rotavirus degrades multiple type interferon
749 receptors to inhibit IFN signaling and protects against mortality from endotoxin in suckling
750 mice. *J Virol*.
751 9. Broquet AH, Hirata Y, McAllister CS, & Kagnoff MF (2011) RIG-I/MDA5/MAVS are required
752 to signal a protective IFN response in rotavirus-infected intestinal epithelium. *J Immunol*
753 186(3):1618-1626.
754 10. Lin JD*, et al.* (2016) Distinct Roles of Type I and Type III Interferons in Intestinal Immunity
755 to Homologous and Heterologous Rotavirus Infections. *PLoS Pathog* 12(4):e1005600.
756 11. Feng N*, et al.* (2008) Role of interferon in homologous and heterologous rotavirus
757 infection in the intestines and extraintestinal organs of suckling mice. *J Virol* 82(15):7578-
758 7590.
759 12. Lundgren O & Svensson L (2001) Pathogenesis of rotavirus diarrhea. *Microbes Infect*
760 3(13):1145-1156.
761 13. Morris AP & Estes MK (2001) Microbes and microbial toxins: paradigms for microbial-
762 mucosal interactions. VIII. Pathological consequences of rotavirus infection and its
763 enterotoxin. *Am J Physiol Gastrointest Liver Physiol* 281(2):G303-310.
764 14. Garrett WS, Gordon JI, & Glimcher LH (2010) Homeostasis and inflammation in the
765 intestine. *Cell* 140(6):859-870.
766 15. Feng N*, et al.* (2011) Roles of VP4 and NSP1 in determining the distinctive replication
767 capacities of simian rotavirus RRV and bovine rotavirus UK in the mouse biliary tract. *J*
768 *Virol* 85(6):2686-2694.
769 16. Feng N, Yasukawa LL, Sen A, & Greenberg HB (2013) Permissive replication of homologous
770 murine rotavirus in the mouse intestine is primarily regulated by VP4 and NSP1. *J Virol*
771 87(15):8307-8316.
772 17. Thapa RJ*, et al.* (2013) Interferon-induced RIP1/RIP3-mediated necrosis requires PKR and
773 is licensed by FADD and caspases. *Proc Natl Acad Sci U S A* 110(33):E3109-3118.

774 18. Apelbaum A, Yarden G, Warszawski S, Harari D, & Schreiber G (2013) Type I interferons
775 induce apoptosis by balancing cFLIP and caspase-8 independent of death ligands. *Mol Cell*
776 *Biol* 33(4):800-814.
777 19. Balachandran S*, et al.* (2000) Alpha/beta interferons potentiate virus-induced apoptosis
778 through activation of the FADD/Caspase-8 death signaling pathway. *J Virol* 74(3):1513-
779 1523.
780 20. Chawla-Sarkar M, Leaman DW, & Borden EC (2001) Preferential induction of apoptosis by
781 interferon (IFN)-beta compared with IFN-alpha2: correlation with TRAIL/Apo2L induction
782 in melanoma cell lines. *Clin Cancer Res* 7(6):1821-1831.
783 21. Feltham R, Vince JE, & Lawlor KE (2017) Caspase-8: not so silently deadly. *Clin Transl*
784 *Immunology* 6(1):e124.
785 22. Wang F*, et al.* (2013) Isolation and characterization of intestinal stem cells based on
786 surface marker combinations and colony-formation assay. *Gastroenterology* 145(2):383-
787 395 e381-321.
788 23. Wurstle ML, Laussmann MA, & Rehm M (2012) The central role of initiator caspase-9 in
789 apoptosis signal transduction and the regulation of its activation and activity on the
790 apoptosome. *Exp Cell Res* 318(11):1213-1220.
791 24. Sen A, Feng N, Ettayebi K, Hardy ME, & Greenberg HB (2009) IRF3 inhibition by rotavirus
792 NSP1 is host cell and virus strain dependent but independent of NSP1 proteasomal
793 degradation. *J Virol* 83(20):10322-10335.
794 25. Sen A, Pruijssers AJ, Dermody TS, Garcia-Sastre A, & Greenberg HB (2011) The early
795 interferon response to rotavirus is regulated by PKR and depends on MAVS/IPS-1, RIG-I,
796 MDA-5, and IRF3. *J Virol* 85(8):3717-3732.
797 26. Sen A, Rott L, Phan N, Mukherjee G, & Greenberg HB (2014) Rotavirus NSP1 protein
798 inhibits interferon-mediated STAT1 activation. *J Virol* 88(1):41-53.
799 27. McComb S*, et al.* (2014) Type-I interferon signaling through ISGF3 complex is required for
800 sustained Rip3 activation and necroptosis in macrophages. *Proc Natl Acad Sci U S A*
801 111(31):E3206-3213.
802 28. Festjens N, Vanden Berghe T, Cornelis S, & Vandenabeele P (2007) RIP1, a kinase on the
803 crossroads of a cell's decision to live or die. *Cell Death Differ* 14(3):400-410.
804 29. Matsuoka Y & Tsujimoto Y (2015) Role of RIP1 in physiological enterocyte turnover in
805 mouse small intestine via nonapoptotic death. *Genes Cells* 20(1):11-28.
806 30. McComb S*, et al.* (2014) Cathepsins limit macrophage necroptosis through cleavage of
807 Rip1 kinase. *J Immunol* 192(12):5671-5678.
808 31. Zhang L*, et al.* (2015) RIP1 Cleavage in the Kinase Domain Regulates TRAIL-Induced NF-
809 kappaB Activation and Lymphoma Survival. *Mol Cell Biol* 35(19):3324-3338.
810 32. Barro M & Patton JT (2005) Rotavirus nonstructural protein 1 subverts innate immune
811 response by inducing degradation of IFN regulatory factor 3. *Proc Natl Acad Sci U S A*
812 102(11):4114-4119.
813 33. Ivashkiv LB & Donlin LT (2014) Regulation of type I interferon responses. *Nat Rev Immunol*
814 14(1):36-49.
815 34. Kim MO, Suh HS, Brosnan CF, & Lee SC (2004) Regulation of RANTES/CCL5 expression in
816 human astrocytes by interleukin-1 and interferon-beta. *J Neurochem* 90(2):297-308.

817 35. Wen X*, et al.* (2010) Predominant interferon-gamma-mediated expression of CXCL9,
818 CXCL10, and CCL5 proteins in the brain during chronic infection with Toxoplasma gondii
819 in BALB/c mice resistant to development of toxoplasmic encephalitis. *J Interferon*
820 *Cytokine Res* 30(9):653-660.
821 36. Sung PS*, et al.* (2017) CXCL10 is produced in hepatitis A virus-infected cells in an IRF3-
822 dependent but IFN-independent manner. *Sci Rep* 7(1):6387.
823 37. Majumder S*, et al.* (1998) p48/STAT-1alpha-containing complexes play a predominant
824 role in induction of IFN-gamma-inducible protein, 10 kDa (IP-10) by IFN-gamma alone or
825 in synergy with TNF-alpha. *J Immunol* 161(9):4736-4744.
826 38. Vargas A*, et al.* (2010) Association between plasma levels of eotaxin (CCL-11) and
827 treatment response to interferon-alpha and ribavirin in HIV/HCV co-infected patients. *J*
828 *Antimicrob Chemother* 65(2):303-306.
829 39. Gasperini S, Calzetti F, Russo MP, De Gironcoli M, & Cassatella MA (1995) Regulation of
830 GRO alpha production in human granulocytes. *J Inflamm* 45(3):143-151.
831 40. Meyer-Hoffert U*, et al.* (2003) Th2- and to a lesser extent Th1-type cytokines upregulate
832 the production of both CXC (IL-8 and gro-alpha) and CC (RANTES, eotaxin, eotaxin-2, MCP-
833 3 and MCP-4) chemokines in human airway epithelial cells. *Int Arch Allergy Immunol*
834 131(4):264-271.
835 41. Chandrasekar B, Deobagkar-Lele M, Victor ES, & Nandi D (2013) Regulation of
836 chemokines, CCL3 and CCL4, by interferon gamma and nitric oxide synthase 2 in mouse
837 macrophages and during Salmonella enterica serovar typhimurium infection. *J Infect Dis*
838 207(10):1556-1568.
839 42. Chiu BC*, et al.* (2003) Cytokine-chemokine networks in experimental mycobacterial and
840 schistosomal pulmonary granuloma formation. *Am J Respir Cell Mol Biol* 29(1):106-116.
841 43. Siegfried A*, et al.* (2013) IFIT2 is an effector protein of type I IFN-mediated amplification
842 of lipopolysaccharide (LPS)-induced TNF-alpha secretion and LPS-induced endotoxin
843 shock. *J Immunol* 191(7):3913-3921.
844 44. Karaghiosoff M*, et al.* (2003) Central role for type I interferons and Tyk2 in
845 lipopolysaccharide-induced endotoxin shock. *Nat Immunol* 4(5):471-477.
846 45. Mahieu T*, et al.* (2006) The wild-derived inbred mouse strain SPRET/Ei is resistant to LPS
847 and defective in IFN-beta production. *Proc Natl Acad Sci U S A* 103(7):2292-2297.
848 46. Sarhan J*, et al.* (2019) Constitutive interferon signaling maintains critical threshold of
849 MLKL expression to license necroptosis. *Cell Death Differ* 26(2):332-347.
850 47. Guo S*, et al.* (2015) Lipopolysaccharide Regulation of Intestinal Tight Junction
851 Permeability Is Mediated by TLR4 Signal Transduction Pathway Activation of FAK and
852 MyD88. *J Immunol* 195(10):4999-5010.
853 48. Gunther C*, et al.* (2011) Caspase-8 regulates TNF-alpha-induced epithelial necroptosis and
854 terminal ileitis. *Nature* 477(7364):335-339.
855 49. Dalet A, Gatti E, & Pierre P (2015) Integration of PKR-dependent translation inhibition
856 with innate immunity is required for a coordinated anti-viral response. *FEBS Lett*
857 589(14):1539-1545.
858 50. Kim HS*, et al.* (2015) STAT1 deficiency redirects IFN signalling toward suppression of TLR
859 response through a feedback activation of STAT3. *Sci Rep* 5:13414.

860 51. Pott J*, et al.* (2011) IFN-lambda determines the intestinal epithelial antiviral host defense.
861 *Proc Natl Acad Sci U S A* 108(19):7944-7949.
862 52. Wang H*, et al.* (2014) Mixed lineage kinase domain-like protein MLKL causes necrotic
863 membrane disruption upon phosphorylation by RIP3. *Mol Cell* 54(1):133-146.
864 53. Duprez L*, et al.* (2011) RIP kinase-dependent necrosis drives lethal systemic inflammatory
865 response syndrome. *Immunity* 35(6):908-918.
866 54. Potten CS & Loeffler M (1990) Stem cells: attributes, cycles, spirals, pitfalls and
867 uncertainties. Lessons for and from the crypt. *Development* 110(4):1001-1020.
868 55. Estornes Y*, et al.* (2014) RIPK1 promotes death receptor-independent caspase-8-
869 mediated apoptosis under unresolved ER stress conditions. *Cell Death Dis* 5:e1555.
870 56. Guerrero CA & Acosta O (2016) Inflammatory and oxidative stress in rotavirus infection.
871 *World J Virol* 5(2):38-62.
872 57. Crawford SE & Estes MK (2013) Viroporin-mediated calcium-activated autophagy.
873 *Autophagy* 9(5):797-798.
874 58. Trujillo-Alonso V, Maruri-Avidal L, Arias CF, & Lopez S (2011) Rotavirus infection induces
875 the unfolded protein response of the cell and controls it through the nonstructural
876 protein NSP3. *J Virol* 85(23):12594-12604.
877 59. Zambrano JL*, et al.* (2011) Rotavirus infection activates the UPR but modulates its activity.
878 *Virol J* 8:359.
879 60. Welz PS*, et al.* (2011) FADD prevents RIP3-mediated epithelial cell necrosis and chronic
880 intestinal inflammation. *Nature* 477(7364):330-334.
881 61. Arnold MM & Patton JT (2011) Diversity of interferon antagonist activities mediated by
882 NSP1 proteins of different rotavirus strains. *J Virol* 85(5):1970-1979.
883 62. Rateitschak K*, et al.* (2010) Mathematical modelling of interferon-gamma signalling in
884 pancreatic stellate cells reflects and predicts the dynamics of STAT1 pathway activity. *Cell*
885 *Signal* 22(1):97-105.
886 63. Swameye I, Muller TG, Timmer J, Sandra O, & Klingmuller U (2003) Identification of
887 nucleocytoplasmic cycling as a remote sensor in cellular signaling by databased modeling.
888 *Proc Natl Acad Sci U S A* 100(3):1028-1033.
889 64. Wiesauer I, Gaumannmuller C, Steinparzer I, Strobl B, & Kovarik P (2015) Promoter
890 occupancy of STAT1 in interferon responses is regulated by processive transcription. *Mol*
891 *Cell Biol* 35(4):716-727.
892 65. Benci JL*, et al.* (2016) Tumor Interferon Signaling Regulates a Multigenic Resistance
893 Program to Immune Checkpoint Blockade. *Cell* 167(6):1540-1554 e1512.
894 66. Bhattacharya S*, et al.* (2014) Triggering ubiquitination of IFNAR1 protects tissues from
895 inflammatory injury. *EMBO Mol Med* 6(3):384-397.
896 67. Ramana CV*, et al.* (2001) Stat1-independent regulation of gene expression in response to
897 IFN-gamma. *Proc Natl Acad Sci U S A* 98(12):6674-6679.
898 68. Lu L*, et al.* (2018) Gene regulation and suppression of type I interferon signaling by STAT3
899 in diffuse large B cell lymphoma. *Proc Natl Acad Sci U S A* 115(3):E498-E505.
900 69. Qing Y & Stark GR (2004) Alternative activation of STAT1 and STAT3 in response to
901 interferon-gamma. *J Biol Chem* 279(40):41679-41685.
902 70. Wang WB, Levy DE, & Lee CK (2011) STAT3 negatively regulates type I IFN-mediated
903 antiviral response. *J Immunol* 187(5):2578-2585.

904 71. Deal EM, Lahl K, Narvaez CF, Butcher EC, & Greenberg HB (2013) Plasmacytoid dendritic
905 cells promote rotavirus-induced human and murine B cell responses. *J Clin Invest*
906 123(6):2464-2474.
907 72. Guerrero CA, Santana AY, & Acosta O (2010) Mouse intestinal villi as a model
908 system for studies of rotavirus infection. *J Virol Methods* 168(1-2):22-30.
909 73. Sen A*, et al.* (2012) Innate immune response to homologous rotavirus infection in the
910 small intestinal villous epithelium at single-cell resolution. *Proc Natl Acad Sci U S A*
911 109(50):20667-20672.
912

Figure 1.

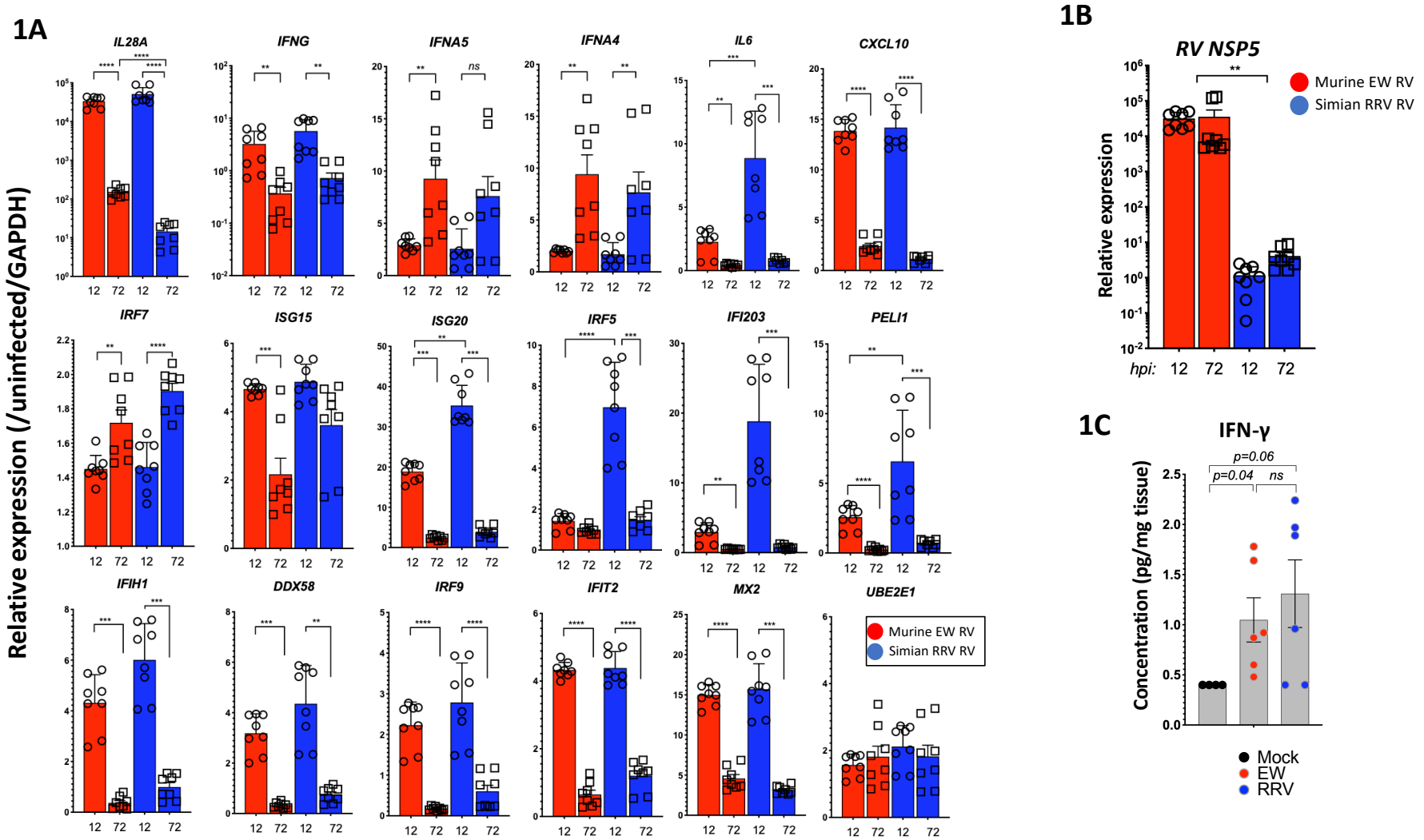
1A
Relative expression (/uninfected/GAPDH)
IL28A
IFNG
IFNA5
IFNA4
IL6
CXCL10
IRF7
ISG15
ISG20
IRF5
IFI203
PELI1
IFIH1
DDX58
IRF9
IFIT2
MX2
UBE2E1
Murine EW RV
Simian RRV RV
1B
RV NSP5
Relative expression
hpi: 12 72 12 72
Murine EW RV
Simian RRV RV
1C
IFN-γ
Concentration (pg/mg tissue)
p=0.06
p=0.04
ns
Mock
EW
RRV

Figure 2.

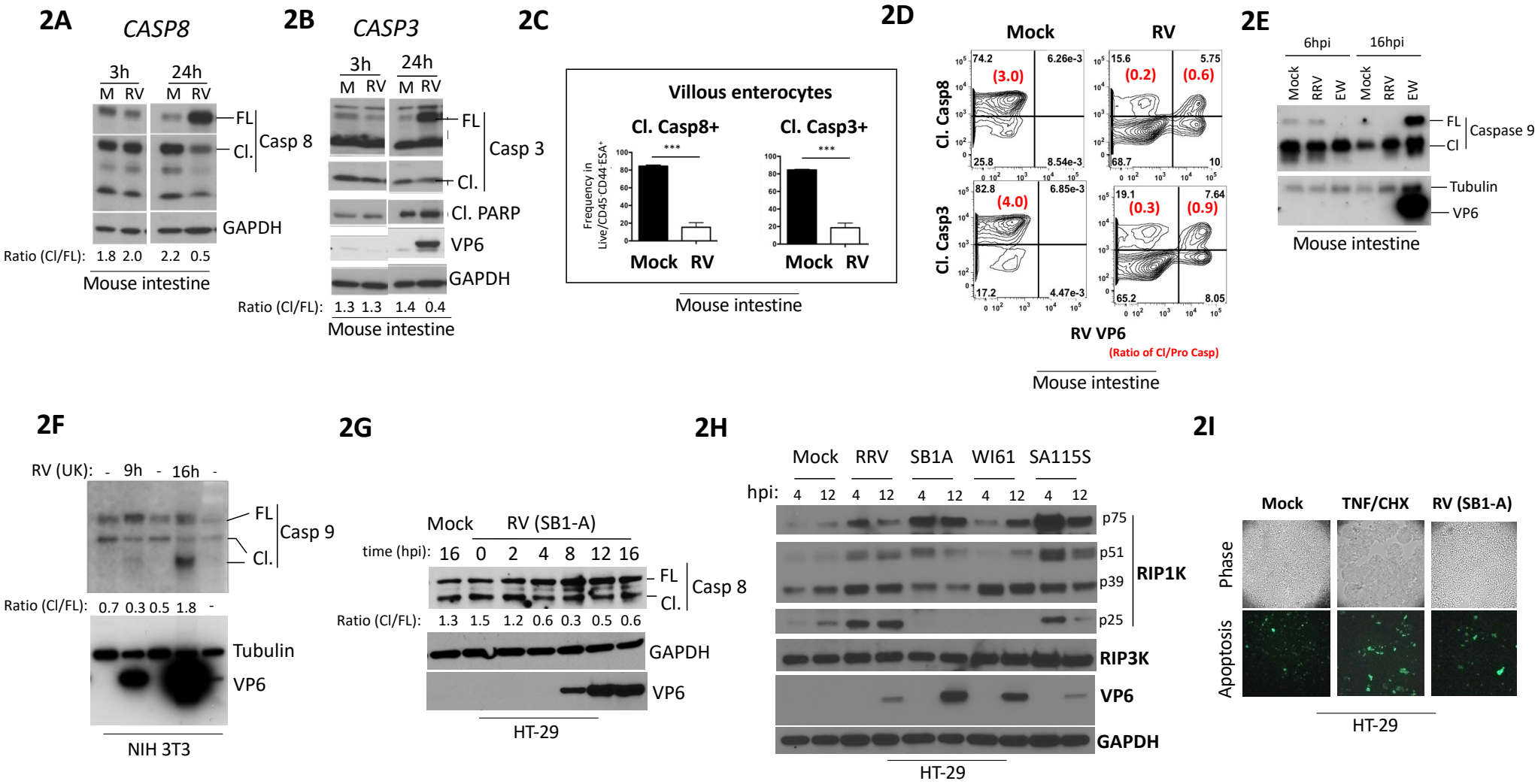
2A
CASP8
3h
24h
M RV M RV
FL
Cl.
Casp 8
GAPDH
Ratio (Cl/FL): 1.8 2.0 2.2 0.5
Mouse intestine
2B
CASP3
3h
24h
M RV M RV
FL
Cl.
Casp 3
Cl. PARP
VP6
GAPDH
Ratio (Cl/FL): 1.3 1.3 1.4 0.4
Mouse intestine
2C
Villous enterocytes
Cl. Casp8+
Cl. Casp3+
Frequency in Live/CD45-CD44-ESA+
***
Mock RV
Mouse intestine
2D
Mock
RV
Cl. Casp8
Cl. Casp3
74.2
6.26e-3
(3.0)
25.8
8.54e-3
15.6
5.75
(0.2)
(0.6)
68.7
10
82.8
6.85e-3
(4.0)
17.2
4.47e-3
19.1
7.64
(0.3)
(0.9)
65.2
8.05
RV VP6
(Ratio of Cl/Pro Casp)
Mouse intestine
2E
6hpi
16hpi
Mock RRV EW Mock RRV EW
FL
Cl
Caspase 9
Tubulin
VP6
Mouse intestine
2F
RV (UK): - 9h - 16h -
FL
Cl.
Casp 9
Ratio (Cl/FL): 0.7 0.3 0.5 1.8 -
Tubulin
VP6
NIH 3T3
2G
Mock
RV (SB1-A)
time (hpi): 16 0 2 4 8 12 16
FL
Cl.
Casp 8
Ratio (Cl/FL): 1.3 1.5 1.2 0.6 0.3 0.5 0.6
GAPDH
VP6
HT-29
2H
Mock RRV SB1A WI61 SA115S
hpi: 4 12 4 12 4 12 4 12 4 12
p75
p51
p39
p25
RIP1K
RIP3K
VP6
GAPDH
HT-29
2I
Mock
TNF/CHX
RV (SB1-A)
Phase
Apoptosis
HT-29

Figure 3.

3A

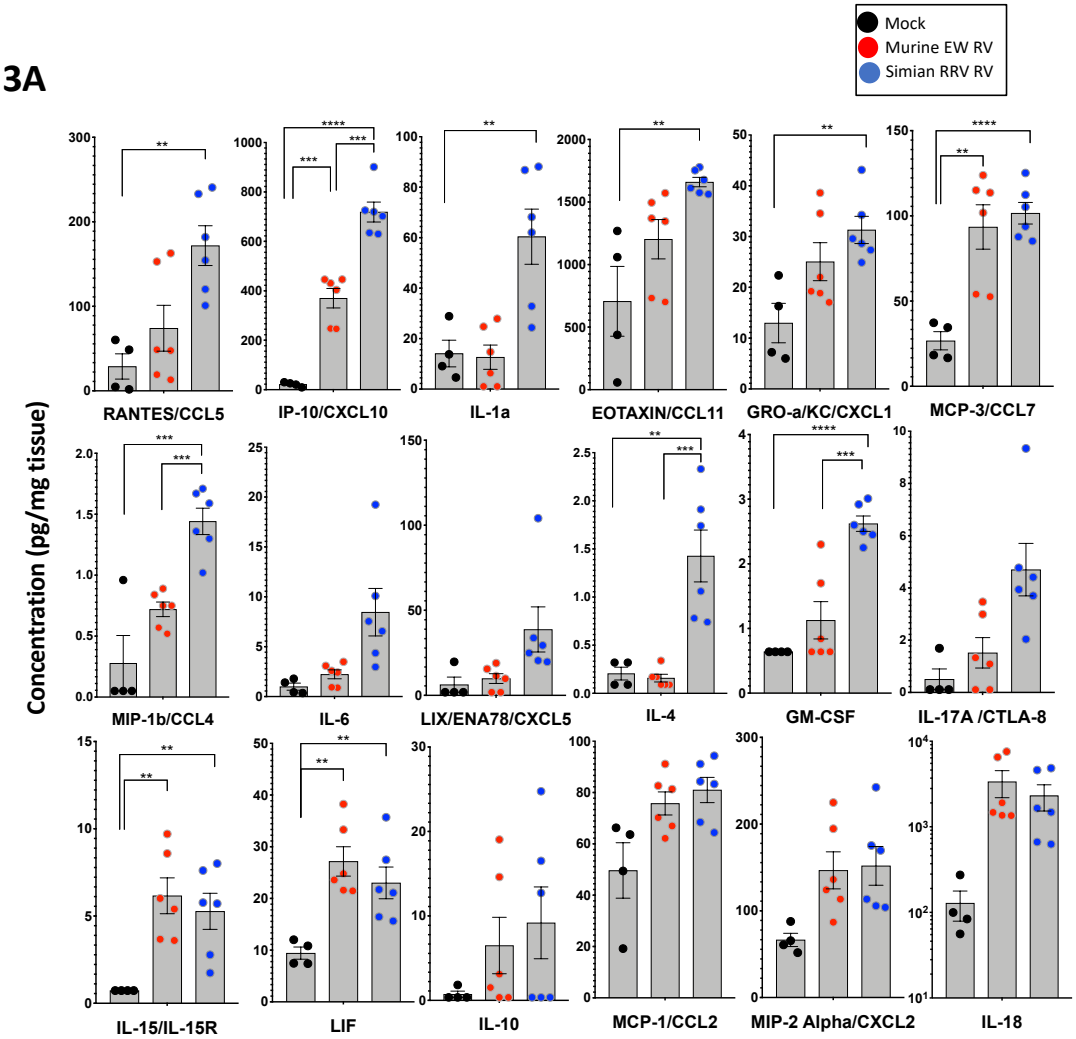

3B

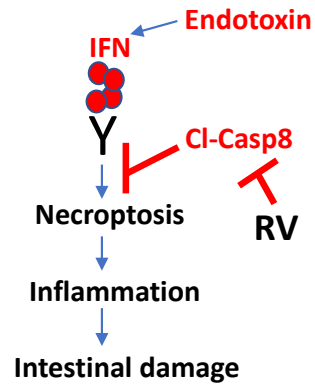

3C

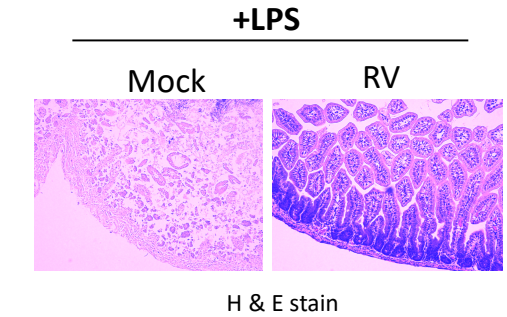

Figure 4.

4A

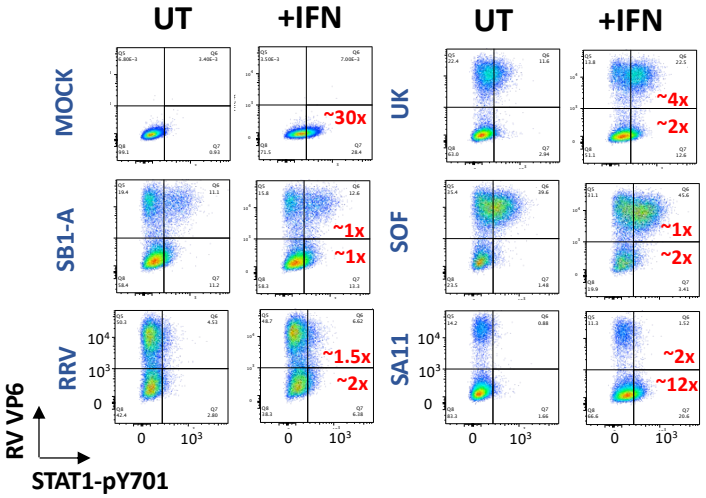

4B

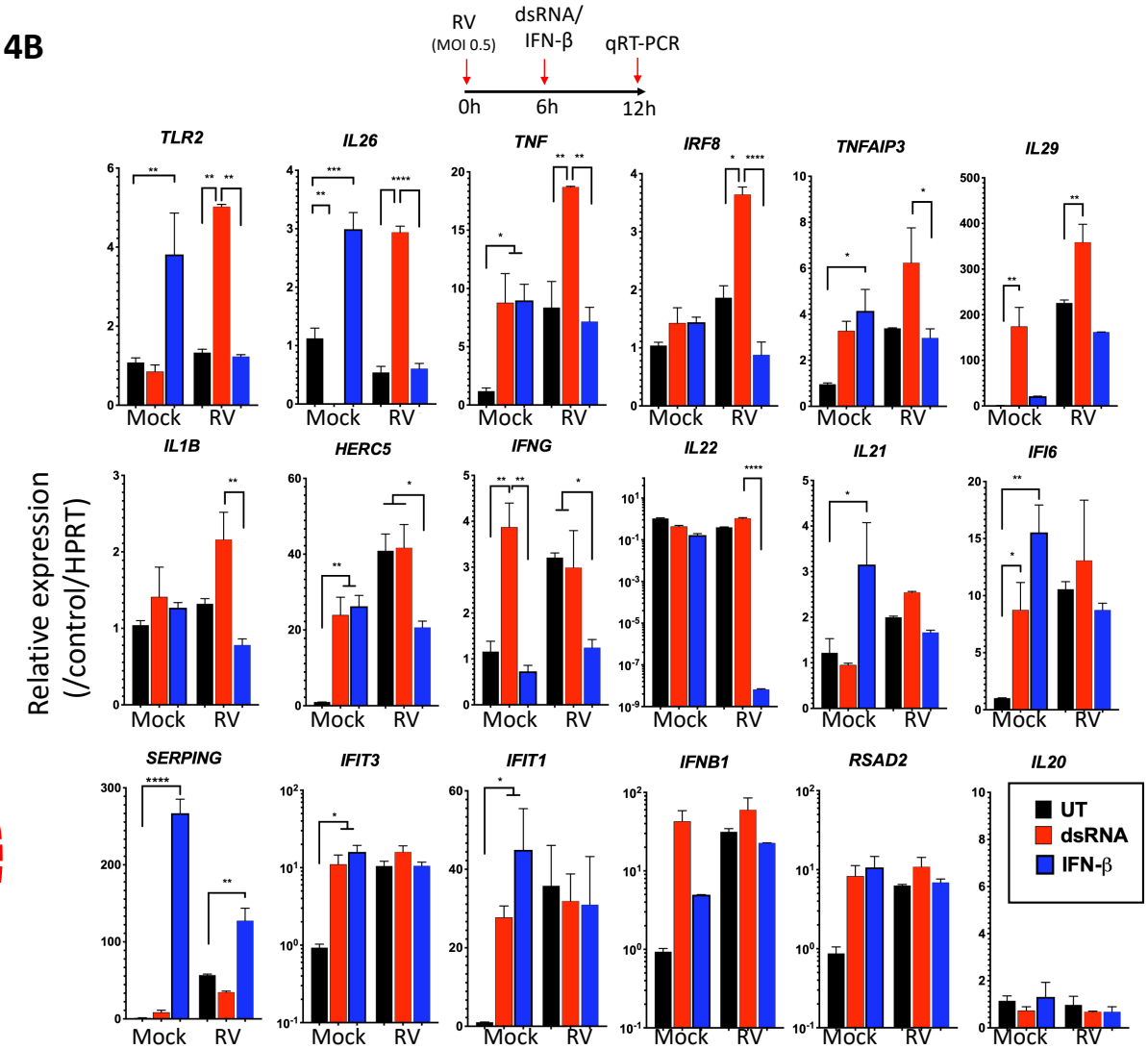

4C

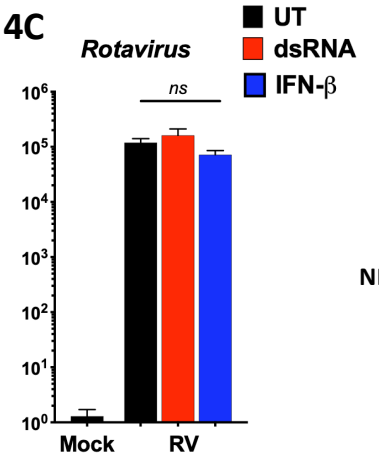

4D

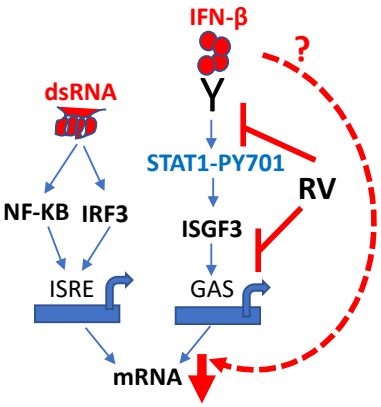

Figure 5.

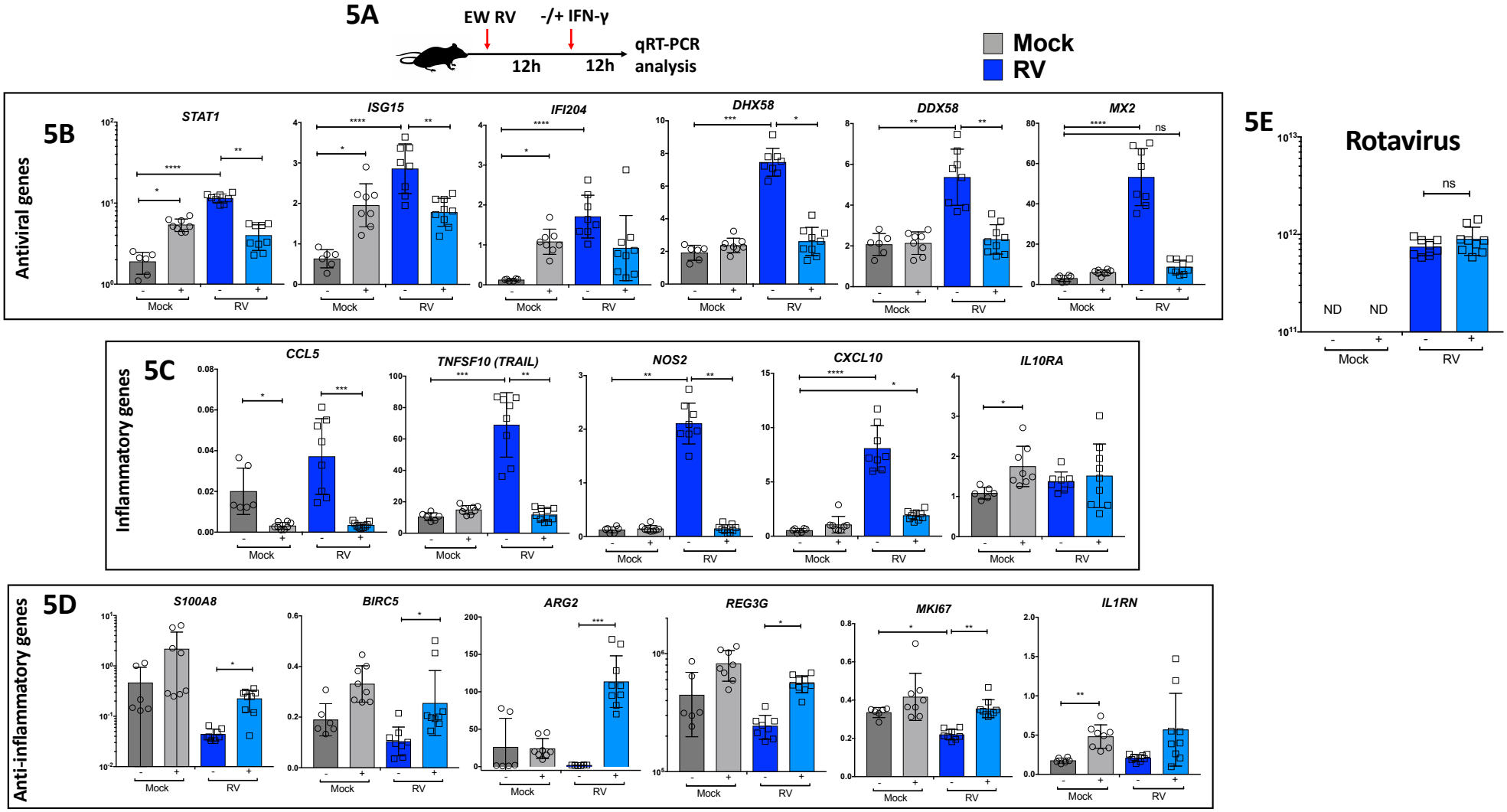
5A
EW RV
-/+ IFN-γ
12h
12h
qRT-PCR analysis
Mock
RV
5B
Antiviral genes
STAT1
ISG15
IFI204
DHX58
DDX58
MX2
5C
Inflammatory genes
CCL5
TNFSF10 (TRAIL)
NOS2
CXCL10
IL10RA
5D
Anti-inflammatory genes
S100A8
BIRC5
ARG2
REG3G
MKI67
IL1RN
5E
Rotavirus
ND
ND
ns
Mock
RV